Proc. Indian Acad. Sci. (Chem. Sci.), Vol. 92, Numbers 4 & 5, August & October 1983, pp. 415–420.

Neutron diffraction using an electron linear accelerator

B T M WILLIS
Materials Physics Division, AERE, Harwell, Oxon OX11 ORA, England

Abstract. The Harwell electron linear accelerator HELIOS has been used for studying the crystal structures of polycrystalline materials by neutron diffraction. Atomic positions and atomic vibrational amplitudes can be determined equally well with the pulsed method as with the more conventional method employing a high-flux nuclear reactor as source. The powder pattern can be indexed more easily with pulsed neutrons.

Keywords. Linear accelerator; neutron diffraction.

1. Introduction

HELIOS, the 136 MeV electron linear accelerator at Harwell, has been used since 1981 to study the physics and chemistry of condensed matter. The accelerator, whose main features have been described by Lynn (1980), may be viewed as a precursor of the more intense Spallation Neutron Source (SNS) which is under construction nearby and due to operate in 1985.

Pulsed neutron techniques are superior to those employing the continuous neutron beam from a nuclear reactor for the study of high-energy excitations in a solid or for the measurement of the structure factors of liquids or amorphous materials where the observations must be made over a wide range of $\sin\Theta/\lambda$. It is less obvious that there are also advantages in using the pulsed method to examine polycrystalline materials by time-of-flight neutron diffraction. We shall illustrate these advantages by describing the results of some experiments with HELIOS and the Harwell back scattering spectrometer (BSS). The main features of the BSS have been described by Windsor *et al* (1977). We shall not consider neutron diffraction from single crystals, although it is in this field that pulsed neutrons are particularly effective in solving the crystallographic phase problem using anomalous dispersion (see Ramaseshan and Narayan 1981).

2. Time-of-flight crystallography

The derivation is given in this section of the basic formulae required for interpreting the time-of-flight diffraction patterns from a polycrystalline sample examined with a pulsed neutron source.

Pulsed neutrons emerge from the target in the 'condensed matter cell' of HELIOS by a two-stage process. Bremsstrahlung radiation with a maximum photon energy equal to the energy of the electron beam (136 MeV) arises from interaction of the electrons with the heavy-metal target; the gamma-rays then take part in a photonuclear reaction to produce fast neutrons. These neutrons are subsequently slowed down to the thermal, or epithermal, range by a moderator consisting of a slab of ordinary water whose moderator time matches the electron pulse length. The pulse width of the moderated

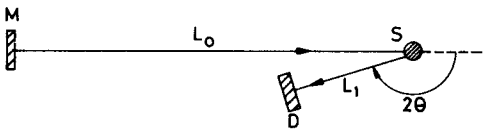

Figure 1. Geometry of back-scattering spectrometer, BSS. *M* is the neutron moderator, *S* the sample and *D* the detector. *D* is coupled to a time-of-flight analyser with 2048 time channels.

neutrons varies with their wavelength, but the mean time spread at the moderator of the neutrons in a single pulse is about 5μsec. This time spread, together with the distance $L = L_0 + L_1$ (see figure 1) travelled by the neutrons from the moderator to the detector, determine the resolution characteristics of the diffraction pattern.

Let t be the time taken by neutrons of velocity v to travel the distance L. Then

$$t = L/v = (Lm_n/h)\lambda, \tag{1}$$

where we have used the de Broglie equation

$$\lambda = h/(m_n v), \tag{2}$$

relating the wavelength λ and the velocity. (h is Planck's constant and m_n the neutron mass.)

Putting the Bragg equation

$$\lambda = 2d \sin \Theta \tag{3}$$

into equation (1), where 2Θ is the scattering angle for the planes of spacing d, gives

$$t = (505{\cdot}54\, L \sin \Theta)d, \tag{4}$$

with t expressed in μsec, L in metres and d in Å units. The path length L in the BSS is 14 m and the scattering angle is 170°, so that the time-of-flight of the neutrons diffracted by planes of 1 Å spacing is a little over 7000 μsec. Clearly, with an initial pulse length of 5 μsec very little uncertainty in the flight time is introduced by the finite pulse length.

Equation (4) shows that the time t is directly proportional to the spacing d. For d values in the range $0{\cdot}5\ A < d < 2{\cdot}5\ A$, the corresponding times are between 3,500 and 17,500 μsec. The neutron counts are recorded in 2048 time channels with a separation of a few μsec between adjacent channels, giving a diffraction pattern such as that shown in figure 2.

Differentiating equation (3) gives

$$\Delta\lambda/\lambda = \cot \Theta\, \Delta\Theta, \tag{5}$$

and so high resolution is achieved by working at a high scattering angle 2Θ in the back scattering region, where $\cot \Theta$ tends to nothing as Θ approaches 90°. If the pattern is recorded for a Θ value in the forward scattering region, then the lines in figure 2 would be less sharply defined.

3. Diffraction at low $\sin\Theta/\lambda$: measurement of d-spacings

The first stage in solving a crystal structure is the measurement of the unit-cell dimensions. Using a polycrystalline sample the crucial requirement is the accurate

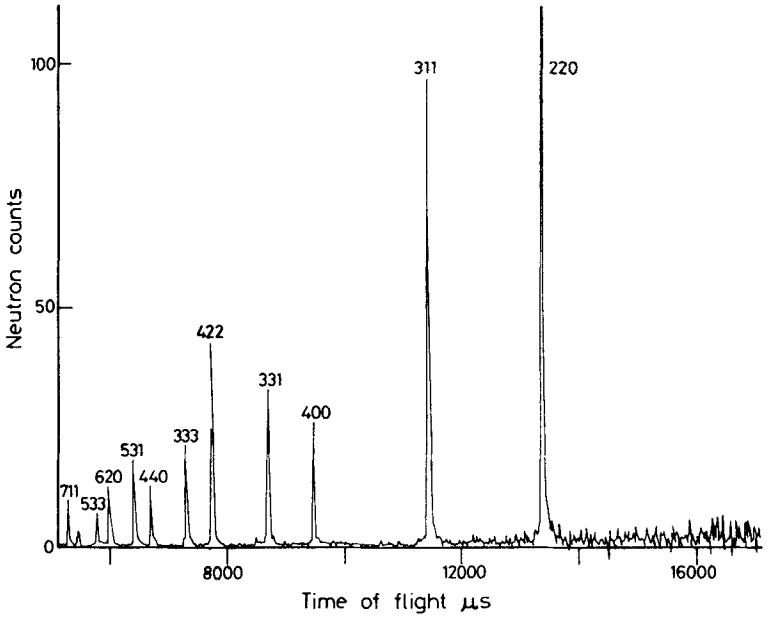

Figure 2. Time-of-flight diffraction pattern of silicon at low Q. The observed spectrum has been ratioed with a vanadium spectrum: vanadium is an incoherent neutron scatterer, whose spectrum gives the wavelength dependence of the incident beam flux.

measurement of the first 20–30 lines of the powder pattern. This point has been emphasised by Shirley (1980): "There can be few fields of endeavour in which careful data preparation is as dramatically rewarded as in computer-based powder indexing. A properly measured pattern is usually solved almost immediately, while mediocre data can run forever". In this context a "properly measured pattern" means that the d-spacings must be known to a few parts in 10,000.

Figure 2 shows a portion of the low sin Θ/λ pattern from silicon, and table 1 indicates the kind of accuracy that can be achieved by measuring the corresponding interplanar spacings. In this table t_{obs} is the time-of-flight at the maximum of each diffraction peak: the neutron counts are recorded in time channels 8 μsec in width, and t_{obs} can be measured to a few tenths of a microsecond by fitting a suitable analytical function (Albinati and Willis 1982) to each peak. The observed d-spacing in the third column of the table was derived from the relation

$$t_{obs} = cd_{obs},$$

where c is an instrumental constant given by (1) and (3) as

$$c = (2m_n/h)\, L \sin \Theta.$$

d_{calc} in the last column of table 1 was calculated from

$$d_{calc} = a_0(h^2 + k^2 + l^2)^{-\frac{1}{2}}$$

with a_0, the cubic lattice parameter of silicon at 20°C, equal to 5·43070 Å. The measured spacings are within 2 parts in 10^4 of the calculated values.

Table 1. Interplanar spacings of silicon by time of flight crystallography.

hkl	t_{obs} (μsec)	d_{obs} (Å)	d_{calc} (Å)
220	13503·5	1·9200	1·9200
311	11515·5	1·6373	1·6374
400	9549·0	1·3577	1·3576
311	8760·4	1·2456	1·2458
422	7796·1	1·1085	1·1085
333	7351·2	1·0452	1·0451
440	6753·2	0·9602	0·9600
531	6455·9	0·9179	0·9179
620	6038·7	0·8586	0·8586
533	5823·3	0·8279	0·8281
444	5512·7	0·7838	0·7838
711	5348·2	0·7604	0·7604
642	5103·2	0·7256	0·7257
731	4972·4	0·7070	0·7070

The exceptionally good resolution $\Delta d/d$ arises in time-of-flight crystallography because the entire diffraction pattern can be collected in back scattering. To obtain comparable resoluton at large d spacings with a reactor source it is necessary to design the diffractometer to give optimum focussing conditions at low values of $\sin\Theta/\lambda$, but this is not normally done as it will spoil the high-$\sin\Theta/\lambda$ portion of the pattern (Hewat 1975).

4. Diffraction at high $\sin\Theta/\lambda$

4.1 *Measurement of atomic positions*

To assess the accuracy of the time-of-flight technique in determining atomic positions, a diffraction pattern was recorded from monoclinic zirconia, ZrO_2, which has a distorted fluorite-type structure. There are three atoms at general positions (not fixed by symmetry) in the unit cell.

Data were collected up to $\sin\Theta/\lambda = 1{\cdot}5$ Å^{-1} with the back-scattering spectrometer, using 15 g of sample and 30 hr of counting time. The data were refined by the Rietveld method (see Albinati and Willis 1982) in which the entire profile of the diffraction pattern is matched to the calculated profile. The final results are shown in figure 3 and

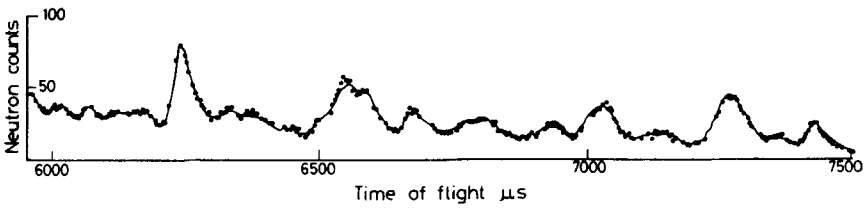

Figure 3. Portion of the time-of-flight diffraction pattern of monoclinic zirconia. Points are the raw data points, and the continuous line the calculated best-fit profile.

Table 2. Fractional atomic coordinates of monoclinic zirconia (space group $P2_1/c$)

	Linac method			Nuclear reactor method		
Atom	x	y	z	x	y	z
Zr	0·2756(4)	0·0393(4)	0·2073(4)	0·276(1)	0·040(1)	0·209(1)
O_I	0·0681(5)	0·3308(4)	0·3453(4)	0·072(2)	0·332(1)	0·344(1)
O_{II}	0·4494(4)	0·7570(5)	0·4802(4)	0·450(2)	0·757(1)	0·478(1)
	$(\sin\Theta/\lambda)_{max} = 1{\cdot}5\ \text{Å}^{-1}$			$(\sin\Theta/\lambda)_{max} = 0{\cdot}8\ \text{Å}^{-1}$		

table 2. Twenty five parameters were varied (including four lattice parameters, three isotropic temperature factors and three coefficients defining the background), but the parameters representing the atomic positions only are given in the table.

The same sample of zirconia has also been analysed by conventional neutron powder diffraction. The high-resoluton neutron powder diffractometer at AERE Harwell was used with the PLUTO nuclear reactor as source, and a Rietveld refinement carried out with a computer program adapted to constant-wavelength, angle-dispersive measurements. These results are listed in table 2 alongside those from the time-of-flight technique.

The numbers in parentheses in table 2 are estimated standard deviations (referring to least significant digits). There is satisfactory agreement between the two sets of coordinates. The greater precision for the coordinates derived by the Linac method is associated with the higher accessible value of $\sin\Theta/\lambda$.

4.2 *Measurement of atomic vibrational amplitudes*

To examine the accuracy to be expected from determing atomic vibrational amplitudes, a polycrystalline sample of thoria was chosen. ThO_2 crystallises in the cubic fluorite arrangement, so that the atomic positions are fixed by symmetry and the vibrational parameters alone are to be derived from the analysis.

Neutron diffraction data were collected in two separate time ranges:

4,000 to 17,500 μsec (with 8 μsec time channels)

and

2,500 to 5,000 μsec (with 2 μsec time channels).

The maximum value of $\sin\Theta/\lambda$ was 0·9 Å^{-1} in the first case and 1·5 Å^{-1} in the second. Analysis was performed by the Rietveld method and the results are given in table 3.

The table shows that by extending $\sin\Theta/\lambda$ from 0·9 Å^{-1} to 1·5 Å^{-1} the uncertainty in the measurement of the atomic vibration parameters is reduced by a factor of two. Compared with a reactor-based instrument, we gain by using the 'hot' neutrons from the epithermal spectrum of HELIOS. The theoretical values in table 2 were derived from a force-constant model used in fitting phonon dispersion relations to neutron inelastic scattering spectra (Dolling *et al* 1965).

5. Conclusions

We have shown that pulsed neutron diffraction, using a back-scattering spectrometer

Table 3. Thermal displacements of thorium dioxide.

Maximum $\sin\Theta/\lambda$ value of (A^{-1})	Number of reflections in pattern	Mean square displacement of thorium (A^2)		Mean square displacement of oxygen (A^2)	
		Measured	Theory	Measured	Theory
0·9	44	2·5 ± 0·6		5·8 ± 0·8	
			2·7		5·4
1·5	130	2·8 ± 0·4		5·4 ± 0·3	

and the Harwell electron linear accelerator, can lead to accurate measurements of *d*-spacings at low values of $\sin\Theta/\lambda$ and of vibrational parameters and atomic coordinates at high values of $\sin\Theta/\lambda$. The performance of the pulsed neutron instrument matches or exceeds that of the best conventional instrument on a nuclear-reactor source. This augurs well for the future of the Spallation Neutron Source, which is under construction at the Rutherford Appleton Laboratory of the UK. The neutron flux of the SNS will be over one hundred times that of HELIOS.

Acknowledgements

It is a pleasure to acknowledge the help received from my Harwell colleagues, Dr R N Sinclair and Dr C G Windsor. The computer program used for the Rietveld analysis of time of flight data was provided by Professor R von Dreele of Arizona State University, USA.

References

Albinati A and Willis B T M 1982 *J. Appl. Crystallogr.* **15** 361
Dolling G, Cowley R A and Woods A D B 1965 *Can. J. Phys.* **43** 1397
Hewat A W 1975 *Nucl. Instrum. Methods* **127** 361
Lynn J E 1980 *Contemp. Phys.* 21 483
Ramaseshan S and Narayan R 1981 *Structural studies in molecular Biology* (eds) G Dodson, J Pickworth and D Sayre (Oxford: University Press) p. 231
Shirley R 1980 NBS *Special Publication No.* 567 361
Windsor C G, Bunce L J, Borcherds P H, Cole I, Fitzmaurice M, Johnson D A G and Sinclair R N 1977 *Nucl. Instrum. Methods* **140** 240.